

# Both T- and L-Type $\text{Ca}^{2+}$ Channels Can Contribute to Excitation-Contraction Coupling in Cardiac Purkinje Cells

Zhengfeng Zhou and Craig T. January

Section of Cardiology, Department of Medicine, The University of Wisconsin, Madison, Wisconsin 53792 USA

**ABSTRACT** Although L-type  $\text{Ca}^{2+}$  channels have been shown to play a central role in cardiac excitation-contraction (E-C) coupling, little is known about the role of T-type  $\text{Ca}^{2+}$  channels in this process. We used the amphotericin B perforated patch method to study the possible role of T-type  $\text{Ca}^{2+}$  current in E-C coupling in isolated canine Purkinje myocytes where both  $\text{Ca}^{2+}$  currents are large. T-type  $\text{Ca}^{2+}$  current was separated from L-type  $\text{Ca}^{2+}$  current using protocols employing the different voltage dependencies of the channel types and their different sensitivities to pharmacological blockade. We showed that  $\text{Ca}^{2+}$  admitted through either T- or L-type  $\text{Ca}^{2+}$  channels is capable of initiating contraction and that the contractions depended on  $\text{Ca}^{2+}$ -induced  $\text{Ca}^{2+}$  release from the sarcoplasmic reticulum (SR). The contractions, however, had different properties. Those initiated by  $\text{Ca}^{2+}$  entry through T-type  $\text{Ca}^{2+}$  channels had a longer delay to the onset of shortening, slower rates of shortening and relaxation, lower peak shortening, and longer time to peak shortening. These differences were present even when L-type  $\text{Ca}^{2+}$  current amplitude, or charge entry, was less than that of T-type  $\text{Ca}^{2+}$  current, suggesting that  $\text{Ca}^{2+}$  entry through the T-type  $\text{Ca}^{2+}$  channel is a less effective signal transduction mechanism to the SR than is  $\text{Ca}^{2+}$  entry through the L-type  $\text{Ca}^{2+}$  channel. We conclude that under our experimental conditions in cardiac Purkinje cells  $\text{Ca}^{2+}$  entry through the T-type  $\text{Ca}^{2+}$  channel can activate cell contraction. However,  $\text{Ca}^{2+}$  entry through the L-type  $\text{Ca}^{2+}$  channel is a more effective signal transduction mechanism. Our findings support the concept that different structural relationships exist between these channel types and the SR  $\text{Ca}^{2+}$  release mechanism.

## INTRODUCTION

Most cardiac myocytes express two types of  $\text{Ca}^{2+}$  channels, the L- and T-types (Bean, 1985; Nilius et al., 1985; Mitra and Morad, 1986; Hirano et al., 1989a; Tseng and Boyden, 1989; Zhou and Lipsius, 1994). The L-type  $\text{Ca}^{2+}$  channel has been closely linked to electrogenic and excitation-contraction (E-C) coupling processes in heart cells (for review see Bers, 1991; Callewaert, 1992; McDonald et al., 1994; G6mes et al., 1997). The T-type  $\text{Ca}^{2+}$  channel has been extensively characterized, yet its role in the heart remains poorly understood. The strongest evidence is that it participates in the electrogenesis of impulse generation in pacemaker cells (Hagiwara et al., 1988; Zhou and Lipsius, 1994). It has been suggested that T-type  $\text{Ca}^{2+}$  channels might participate in E-C coupling (Mitra and Morad, 1986; Le Grand et al., 1990), but evidence showing this directly is lacking.

In cardiac cells, T-type  $\text{Ca}^{2+}$  current density is largest in Purkinje and atrial cell types, whereas in ventricular cells its density normally is small. T-type  $\text{Ca}^{2+}$  current density, however, is reported to be increased in ventricular cells isolated from chronically hypertensive animals (Nuss and Houser, 1993), in genetic models of cardiomyopathy (Sen and Smith, 1994), by the drug ouabain (Le Grand et al., 1990), in atrial postnatal development (Xu and Best, 1992),

and in dedifferentiated cultured ventricular heart cells (Fares et al., 1996).

In this report, we tested the postulate that  $\text{Ca}^{2+}$  entry via the T-type  $\text{Ca}^{2+}$  channel could participate in E-C coupling in some heart cells. We studied cardiac Purkinje cells, where both T- and L-type  $\text{Ca}^{2+}$  current densities are large, and we used the perforated patch-clamp technique to minimize the effects of cell dialysis-induced current and contraction rundown. Under these experimental conditions,  $\text{Ca}^{2+}$  admitted through either T- or L-type  $\text{Ca}^{2+}$  channels was capable of initiating cell contraction; however, the contractions had different properties. Our findings may have implications for structural relationships of these channels and the sarcoplasmic reticulum (SR)  $\text{Ca}^{2+}$  release channel.

## MATERIALS AND METHODS

### Single Purkinje cells

Single canine Purkinje cells were isolated enzymatically (Sheets et al., 1983). Cells were studied in a heated microchamber mounted on an inverted microscope (Nikon). All experiments were performed at  $30 \pm 1^\circ\text{C}$ .

### Perforated patch-clamp recording technique

Ionic currents were recorded in whole-cell configuration using the amphotericin B perforated patch method as described by Rae and co-workers (Rae et al., 1990; see also Horn and Marty, 1988; Zhou et al., 1995). Amphotericin B (60 mg/ml; Sigma Chemical Co., St. Louis, MO) was first dissolved in dimethylsulfoxide and then added to the internal pipette solution at a final concentration of 240  $\mu\text{g/ml}$ . The internal pipette solution contained (in mM) 100 cesium glutamate, 40 CsCl, 1.0  $\text{MgCl}_2$ , 1.0 EGTA,

Received for publication 29 October 1997 and in final form 7 January 1998.

Address reprint requests to Dr. Craig T. January, Cardiology Section H6/352, 600 Highland Avenue, Madison WI 53792-3248. Tel.: 608-262-5291; Fax: 608-263-0405; E-mail: ctj@medicine.wisc.edu.

© 1998 by the Biophysical Society

0006-3495/98/04/1830/10 \$2.00

and 5 HEPES and was titrated with CsOH to pH 7.2. Because EGTA was included in the pipette solution, inadvertent rupture of the cell membrane within the pipette tip (creating a conventional ruptured patch whole-cell configuration with cell dialysis) was evident as the rapid disappearance of cell contraction and the gradual rundown of  $\text{Ca}^{2+}$  current amplitude. For the formation of a gigaseal, the tip of the pipette was filled with amphotericin-free pipette solution and the pipette was backfilled with the amphotericin-B-containing pipette solution. With the amphotericin B method, the access resistances usually were 4–8 M $\Omega$ . After electronic compensation, this is a suitable access resistance for voltage clamp, and voltage deviation at peak ionic current in these experiments typically should not exceed 1–2 mV. The junction potential was nulled to zero current before the pipette was sealed to the cell. With insertion of amphotericin into the cell membrane after gigaseal formation, a small-amplitude diffusion potential of a few millivolts through amphotericin channels appears (for discussion see Barry and Calc, 1994). Records were not corrected for these small-amplitude voltage shifts.

In most experiments, the pipette was sealed to the cell membrane near the center of the cell and electrical access to the cell interior was obtained in  $\text{Na}^+$ -containing (137 mM NaCl, see Zhou et al., 1995; Vorperian et al., 1996) Tyrode's solution.  $\text{Na}^+$  in the bath solution was removed by first switching to  $\text{Na}^+$ - and  $\text{Ca}^{2+}$ -free solution (NaCl replaced with TEA-Cl, nominally  $\text{Ca}^{2+}$ -free) to minimize  $\text{Ca}^{2+}$  loading (Bers et al., 1990). The bath solution was then switched to a  $\text{Na}^+$ - and  $\text{K}^+$ -free solution containing (in mM) 140 TEA-Cl, 2,4-aminopyridine, 1.8  $\text{CaCl}_2$  (or  $\text{BaCl}_2$ ), 1  $\text{MgCl}_2$ , 10 glucose, 10 HEPES (pH adjusted to 7.4 with TEA-OH), and 0.01–0.02 tetrodotoxin (Calbiochem, La Jolla, CA). In this solution,  $\text{Na}^+$ ,  $\text{K}^+$ , and Na-Ca exchange currents should be suppressed, permitting the recording of T- and L-type  $\text{Ca}^{2+}$  channel currents. When used,  $\text{Cd}^{2+}$  (10–200  $\mu\text{M}$ ) was added as  $\text{CdCl}_2$ ,  $\text{Ni}^{2+}$  (100–400  $\mu\text{M}$ ) was added as  $\text{NiCl}_2$ , nifedipine (1–10  $\mu\text{M}$ ) was added from a 10 mM ethanol stock solution, nitrendipine (10  $\mu\text{M}$ ) was added from a 10 mM dimethylsulfoxide stock solution, and D-600 (1–10  $\mu\text{M}$ ) was added from a 10 mM distilled water stock solution.

Patch electrodes were fabricated as previously described (Hirano et al., 1992; Vorperian et al., 1996). Voltage clamp was obtained using a patch-clamp amplifier (Axopatch 1D, Axon Instruments) under the control of pCLAMP software (Version 5.5.1, Axon Instruments).

## Cell shortening

Contraction was measured at one end of isotonic contracting cells monitored using a CCD video camera (Hamamatsu) mounted on the microscope sideport and a single raster-line scanning cell edge detection technique (Steadman et al., 1988). Shortening records were not corrected for the small amplitude time delays found with this technique (Spurgeon et al., 1990).

Purkinje cells retain stable large-amplitude contractions when stimulated from rest or at low frequencies (see January and Fozzard, 1990), which is different from ventricular cells. Therefore, voltage clamp steps were applied at 0.1 Hz. To examine SR loading at this rate, up to five conditioning pulses were applied (steps to +20 mV for 300 ms at 1 Hz to activate both L- and T-type  $\text{Ca}^{2+}$  current) before applying the test step. Conditioning steps in our Purkinje cells did not alter the contraction amplitude findings; therefore most experiments did not use conditioning steps.

Voltage clamp and cell shortening data were digitized on-line using pCLAMP software and stored on a laboratory computer for subsequent analysis. With the amphotericin B perforated patch clamp method, we have shown that stable  $\text{Ca}^{2+}$  current and cell contraction amplitudes may be recorded for up to 1 h without rundown (Zhou et al., 1995).

## Experimental protocols

T- and L-type  $\text{Ca}^{2+}$  currents were separated by their different voltage-dependent and ion substitution properties and by different sensitivities to pharmacological agents that block  $\text{Ca}^{2+}$  channels. These approaches per-

mitted the unambiguous separation of T-type  $\text{Ca}^{2+}$  current from L-type  $\text{Ca}^{2+}$  current (Hirano et al., 1989a). Peak  $\text{Ca}^{2+}$  currents were measured as the difference between the inward peak and the current remaining at the end of the voltage step. For L-type  $\text{Ca}^{2+}$  current, this method may result in a small underestimate of current amplitude arising from non-inactivating current present at the end of a voltage step. The magnitude of error, however, is small (Hirano et al., 1992), and measuring L-type  $\text{Ca}^{2+}$  current as the  $\text{Cd}^{2+}$ - and  $\text{Ni}^{2+}$ -sensitive current (see Fig. 3) gives similar results. Data are shown without capacitance or leak correction. Where appropriate, data are given as mean  $\pm$  SEM.

Cells meeting the following criteria were studied: 1) access resistance (before compensation) was  $\leq 8$  M $\Omega$  with small leak current, 2) L- and T-type  $\text{Ca}^{2+}$  currents did not rundown, 3) shortening amplitude was stable without contraction rundown, and 4) spontaneous contractions were absent during experiments.

## RESULTS

### Separation of T-type from L-type $\text{Ca}^{2+}$ current in perforated patch-clamped cells

The voltage protocol used to separate T- from L-type  $\text{Ca}^{2+}$  currents by their different voltage-dependent properties is shown in Fig. 1. In Fig. 1 A, voltage clamp steps were applied that selectively activate T-type  $\text{Ca}^{2+}$  current (holding potential of  $-80$  mV with depolarizing steps to voltages between  $-50$  and  $-30$  mV) or L-type  $\text{Ca}^{2+}$  current (holding potential of  $-40$  or  $-50$  mV with depolarizing steps to more positive voltages) or that activate both T- and L-type  $\text{Ca}^{2+}$  current (holding potential of  $-80$  mV with steps to voltages positive to  $-30$  mV). The difference current, obtained by subtracting the currents elicited from the different holding potentials, shows T-type  $\text{Ca}^{2+}$  current. Fig. 1 B shows the peak  $I$ - $V$  plot for the currents shown above. The  $I$ - $V$  plots show that the threshold voltage for L-type  $\text{Ca}^{2+}$  current is between  $-30$  and  $-20$  mV, whereas the threshold voltage for T-type  $\text{Ca}^{2+}$  current is close to  $-50$  mV. For steps to positive voltages, L-type  $\text{Ca}^{2+}$  current was the dominant current. To confirm further the voltage-dependent separation of T- from L-type  $\text{Ca}^{2+}$  current in the perforated patch configuration, in four cells the protocol was repeated after the bath solution charge carrier was changed from  $\text{Ca}^{2+}$  to  $\text{Ba}^{2+}$  (see Hirano et al., 1989a). Under these conditions,  $\text{Ca}^{2+}$ -dependent inactivation of L-type current is abolished with slowing of the L-type  $\text{Ca}^{2+}$  current decay, which facilitates the separation of T- and L-type  $\text{Ca}^{2+}$  currents. With  $\text{Ba}^{2+}$ , the voltage dependence of L- and T-type  $\text{Ca}^{2+}$  currents was similar to that found with  $\text{Ca}^{2+}$  (data not shown), and this agrees with previous results in Purkinje cells (Hirano et al., 1989a).

### Cell contraction with $\text{Ca}^{2+}$ entry through T- and L-type channels

Fig. 2 A shows examples of cell shortening records obtained using the voltage clamp protocol employed in Fig. 1. Voltage clamp steps of 600 ms duration were applied to different voltages in 10-mV increments from a holding potential of  $-80$  or  $-50$  mV at 0.1 Hz. From a holding potential of  $-80$

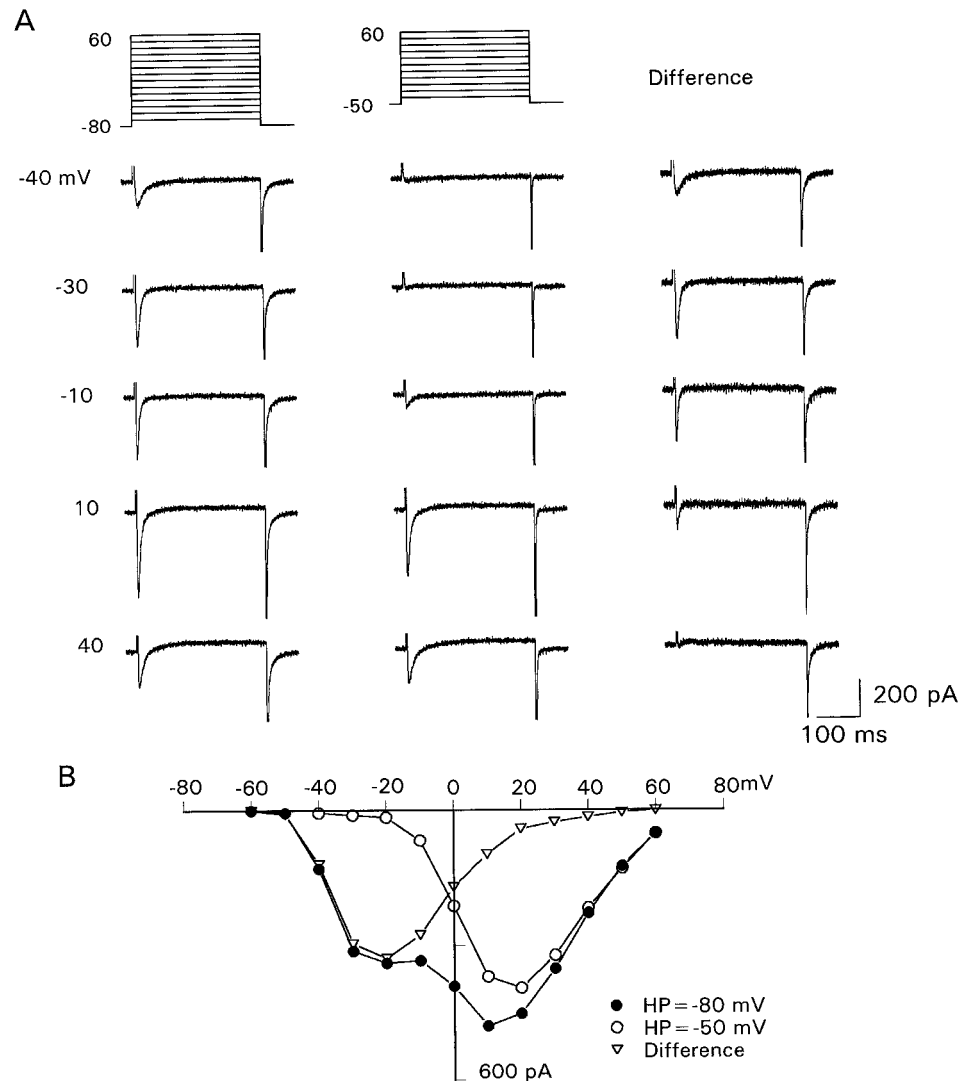


**FIGURE 1** Separation of T- and L-type  $\text{Ca}^{2+}$  currents by voltage in a cell studied using the perforated patch clamp method. (A) Original current traces obtained with depolarizing voltage steps from holding potentials (HP) of  $-80$  and  $-50$  mV are shown along with difference current traces. (B) Peak  $I$ - $V$  plots. See text for details.

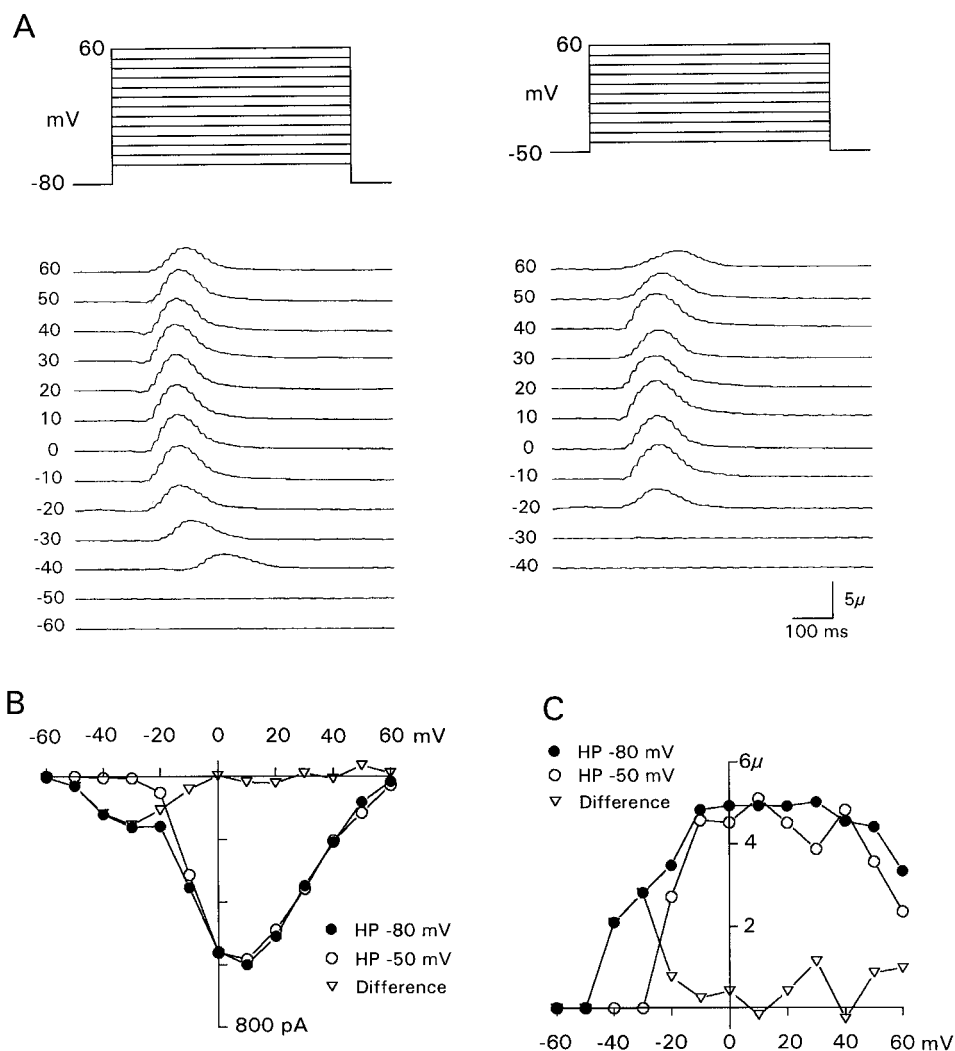
mV, depolarizing steps to  $-50$  mV or more negative voltages did not initiate cell shortening, whereas steps to  $-40$  mV or more positive voltages initiated cell shortening. From a holding potential of  $-50$  mV, depolarizing steps to  $-40$  and  $-30$  mV did not initiate cell shortening, whereas depolarizing steps to  $-20$  mV or more positive voltages initiated cell shortening. Fig. 2 B shows  $I$ - $V$  plots for the peak  $\text{Ca}^{2+}$  currents at the different holding potentials and for the difference current in the same cell. From a holding potential of  $-80$  mV, the  $I$ - $V$  plot has a biphasic shape. T-type  $\text{Ca}^{2+}$  current was activated with voltage steps to between approximately  $-50$  and  $-20$  mV with the peak T-type  $\text{Ca}^{2+}$  current amplitude at  $-30$  mV. With steps to more positive voltages from both holding potentials, a larger-amplitude L-type  $\text{Ca}^{2+}$  current was present with the current amplitude maximal for voltage steps to  $+10$  mV. Fig. 2 C shows peak shortening-voltage plots for the same cell. From a holding potential of  $-80$  mV, the threshold voltage for initiating contraction was between  $-50$  and  $-40$  mV, close to the threshold voltage of T-type  $\text{Ca}^{2+}$  current. In contrast, from a holding potential of  $-50$  mV, where only L-type

$\text{Ca}^{2+}$  current is elicited, the threshold voltage for initiating cell contraction was between  $-30$  and  $-20$  mV, which is close to the threshold voltage of L-type  $\text{Ca}^{2+}$  current. The shortening difference record, obtained by subtracting the peak shortening records at both holding potentials, may represent cell contraction associated with  $\text{Ca}^{2+}$  entry as T-type  $\text{Ca}^{2+}$  current. The shortening difference record was maximal for voltage steps to  $-30$  mV, which is the same voltage at which peak T-type  $\text{Ca}^{2+}$  current amplitude was reached. The peak shortening-voltage plot also shows that shortening was voltage dependent and that at more positive voltages peak cell shortening declined. Similar findings, showing the initiation of cell contraction with voltage steps that selectively activate T-type  $\text{Ca}^{2+}$  current, were obtained in a total of 21 cells.

#### Effect of $\text{Ca}^{2+}$ channel blockade

The dependence of cell shortening on surface membrane  $\text{Ca}^{2+}$  channel activation was shown several ways. In  $\text{Ca}^{2+}$ -

FIGURE 2 T- and L-type  $\text{Ca}^{2+}$  currents and cell shortening in a cardiac Purkinje cell. (A) Cell shortening (upward deflection) was recorded while cells were held at  $-80$  (left traces) or  $-50$  (right traces) mV and clamped to the voltages shown. (B) Peak  $I$ - $V$  plots and difference current trace. (C) Peak shortening-voltage plots and difference shortening trace for the same cell. From a holding potential (HP) of  $-80$  mV, depolarizing clamp steps to voltages between  $-50$  and  $-30$  mV elicited T-type  $\text{Ca}^{2+}$  current and cell shortening. Steps to more positive voltages elicited similar amplitude L-type  $\text{Ca}^{2+}$  currents and cell shortening.



containing bath solution, cell shortening could be blocked by the addition of both  $\text{Ni}^{2+}$  ( $400 \mu\text{M}$ ) and  $\text{Cd}^{2+}$  ( $200 \mu\text{M}$ ), which at these concentrations block nearly completely T- and L-type  $\text{Ca}^{2+}$  currents (Hirano et al., 1989a). Example records are shown in Fig. 3. Voltage steps to  $-40$  and  $+20$  mV were applied to elicit T- or mostly L-type  $\text{Ca}^{2+}$  current and cell shortening (left panels). The subsequent records were obtained 10 min later after the addition of  $\text{Ni}^{2+}$  and  $\text{Cd}^{2+}$  to the bath and show block of T- and L-type  $\text{Ca}^{2+}$  current and cell shortening. Similarly, eliminating  $\text{Ca}^{2+}$  from the bath solution (e.g., nominally  $\text{Ca}^{2+}$ -free, data not shown) abolished T- and L-type  $\text{Ca}^{2+}$  currents and cell shortening, and the replacement of  $\text{Ca}^{2+}$  by  $\text{Ba}^{2+}$  also abolished cell shortening (data not shown).

We studied the separation of T- from L-type  $\text{Ca}^{2+}$  current using several blockers of L-type  $\text{Ca}^{2+}$  channels. Ionic blockers, such as  $\text{Cd}^{2+}$  or  $\text{Ni}^{2+}$ , in moderate concentrations ( $10$ – $100 \mu\text{M}$ ), lack high selectivity in our cells (see Hirano et al., 1989a), which we confirmed in the present experiments. Organic  $\text{Ca}^{2+}$  channel blockers, including the dihydropyridines nifedipine ( $1$ – $10 \mu\text{M}$ ) and nitrendipine ( $10 \mu\text{M}$ ) and the phenylalkylamine D-600 ( $1$ – $10 \mu\text{M}$ ), while

having greater selectivity for block of L-type  $\text{Ca}^{2+}$  channels, also have complex voltage- and use-dependent blocking properties (Bean, 1984; McDonald et al., 1984; Sanguinetti and Kass, 1984; Hirano et al., 1989a; Kamp et al., 1998). At the more negative holding potentials required in these experiments to activate T-type  $\text{Ca}^{2+}$  current, L-type  $\text{Ca}^{2+}$  channel block by these compounds is incomplete. We therefore studied combinations of  $\text{Ca}^{2+}$  channel blockers. When a low concentration of  $\text{Cd}^{2+}$  ( $10 \mu\text{M}$ ) was added to a solution containing nifedipine ( $10 \mu\text{M}$ ), nearly complete suppression of L-type  $\text{Ca}^{2+}$  current with minimal effects on T-type  $\text{Ca}^{2+}$  current was obtained. Example records are shown in Fig. 4. In Fig. 4 A, cell shortening and membrane current records are shown from one cell for voltage steps to  $-30$  mV (activates T-type  $\text{Ca}^{2+}$  current) and to  $+30$  mV (activates mostly L-type  $\text{Ca}^{2+}$  current). The records on the left show control data, whereas the records on the right show the effects of  $10 \mu\text{M}$  nifedipine plus  $10 \mu\text{M}$   $\text{Cd}^{2+}$ . With this combination, T-type  $\text{Ca}^{2+}$  current amplitude was minimally decreased, whereas L-type  $\text{Ca}^{2+}$  current was nearly completely abolished. Fig. 4 B shows averaged peak  $I$ - $V$  plots obtained from four cells studied under control

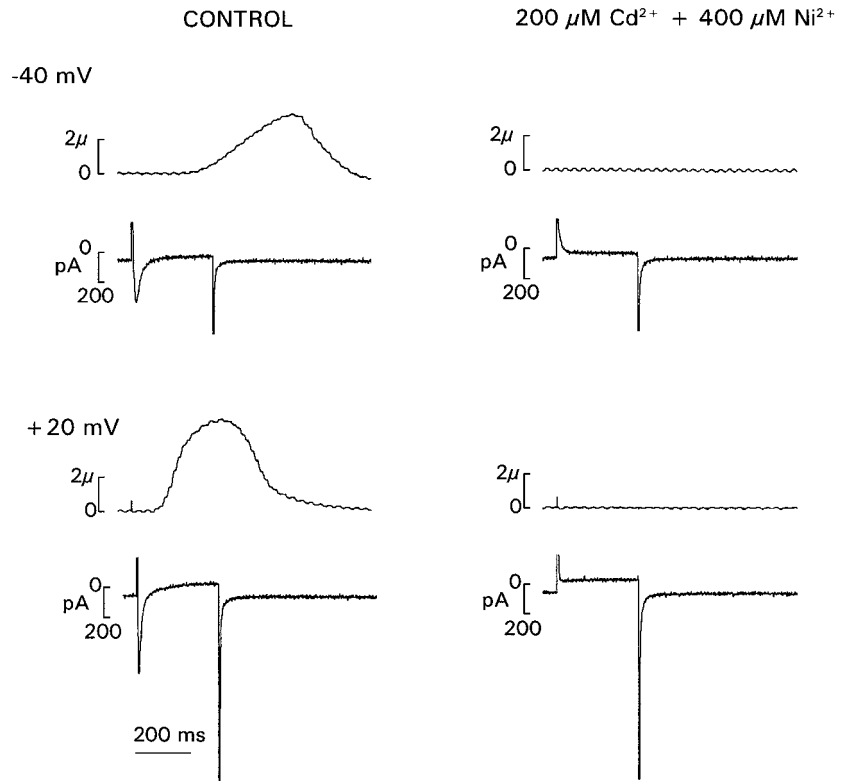


FIGURE 3 Effect of high concentrations of  $\text{Ni}^{2+}$  and  $\text{Cd}^{2+}$ . The left panels show contractions and  $\text{Ca}^{2+}$  currents elicited by clamp steps to  $-40$  mV (to elicit T-type  $\text{Ca}^{2+}$  current) or  $+20$  mV (to elicit mostly L-type  $\text{Ca}^{2+}$  current) from a holding potential of  $-80$  mV in control solution. The right panels show that the addition to the bath solution of  $200 \mu\text{M Cd}^{2+}$  plus  $400 \mu\text{M Ni}^{2+}$  abolished both the  $\text{Ca}^{2+}$  currents and their contractions.

conditions and after exposure to the combination of nifedipine and  $\text{Cd}^{2+}$  (holding potential of  $-80$  mV). The control  $I$ - $V$  plot shows the biphasic shape expected with T- and L-type  $\text{Ca}^{2+}$  currents (see Fig. 1). The  $I$ - $V$  plot in the presence of nifedipine plus  $\text{Cd}^{2+}$  shows block of L-type  $\text{Ca}^{2+}$  current with minimal suppression of the T-type component. At the most positive voltages, little inward  $\text{Ca}^{2+}$  current remained consistent with nearly complete block of L-type  $\text{Ca}^{2+}$  channels. Thus, the remaining current should represent nearly pure, unblocked T-type  $\text{Ca}^{2+}$  current (see below). Fig. 4 C shows peak shortening-voltage plots for the same cells for control conditions and after exposure to nifedipine and  $\text{Cd}^{2+}$ . Under both conditions, the threshold voltage for initiating contraction was close to  $-50$  mV, near that of the T-type  $\text{Ca}^{2+}$  current. The major differences were that, in the presence of nifedipine and  $\text{Cd}^{2+}$ , peak shortening amplitude was less, with the greatest shortening occurring at more negative voltages, and at more positive voltages, cell shortening was abolished. Data from Fig. 4, B and C, are replotted in Fig. 4 D, where the  $I$ - $V$  and peak shortening-voltage plots obtained in the presence of the nifedipine and  $\text{Cd}^{2+}$  combination were superimposed. The voltage dependence of the  $I$ - $V$  plot, which represents nearly pure T-type  $\text{Ca}^{2+}$  current, and the shape of the peak shortening-voltage plot are nearly identical.

Additional evidence of selective suppression of L-type  $\text{Ca}^{2+}$  current with the combination of  $10 \mu\text{M}$  nifedipine plus  $10 \mu\text{M Cd}^{2+}$  is shown in Fig. 5. Current decays from one cell are shown inverted and plotted as the logarithmic transform. Fig. 5 A shows two current decay records for

voltage steps from  $-80$  to  $-30$  mV to selectively activate T-type  $\text{Ca}^{2+}$  channels. The larger amplitude current trace was recorded for control conditions and the other current trace was recorded after the addition to the bath of  $10 \mu\text{M}$  nifedipine plus  $10 \mu\text{M Cd}^{2+}$ . For both current traces, the semilogarithmic plot of the current decay is linear with similar time constants, consistent with previously reported findings (see Hirano et al., 1989b). The data also show that the combination of nifedipine and  $\text{Cd}^{2+}$  caused only a small decrease in T-type  $\text{Ca}^{2+}$  current amplitude. Fig. 5 B shows two current traces obtained for voltage steps from  $-80$  to  $0$  mV, which activates both T- and L-type  $\text{Ca}^{2+}$  currents. The larger amplitude current trace was recorded for control conditions whereas the smaller amplitude current trace was recorded after the addition to the bath of  $10 \mu\text{M}$  nifedipine plus  $10 \mu\text{M Cd}^{2+}$ . Several effects occurred. 1) Peak current amplitude was markedly reduced by the combination. 2) The multiexponential current decay recorded for control conditions was converted to a single exponential decay as would be expected with block of L-type  $\text{Ca}^{2+}$  channels leaving T-type  $\text{Ca}^{2+}$  channels unblocked. 3) The single exponential decay is more rapid at  $0$  mV when compared with that present at  $-30$  mV (see Hirano et al., 1989b). Although activation of a small number of L-type  $\text{Ca}^{2+}$  channels cannot be excluded, the data support the conclusion that block of L-type  $\text{Ca}^{2+}$  current by the combination of  $10 \mu\text{M}$  nifedipine and  $10 \mu\text{M Cd}^{2+}$  is nearly complete and that the effects on T-type  $\text{Ca}^{2+}$  current are small. These results provide further support for the findings shown in Fig. 4 that the  $\text{Ca}^{2+}$  current and cell shortening remaining after



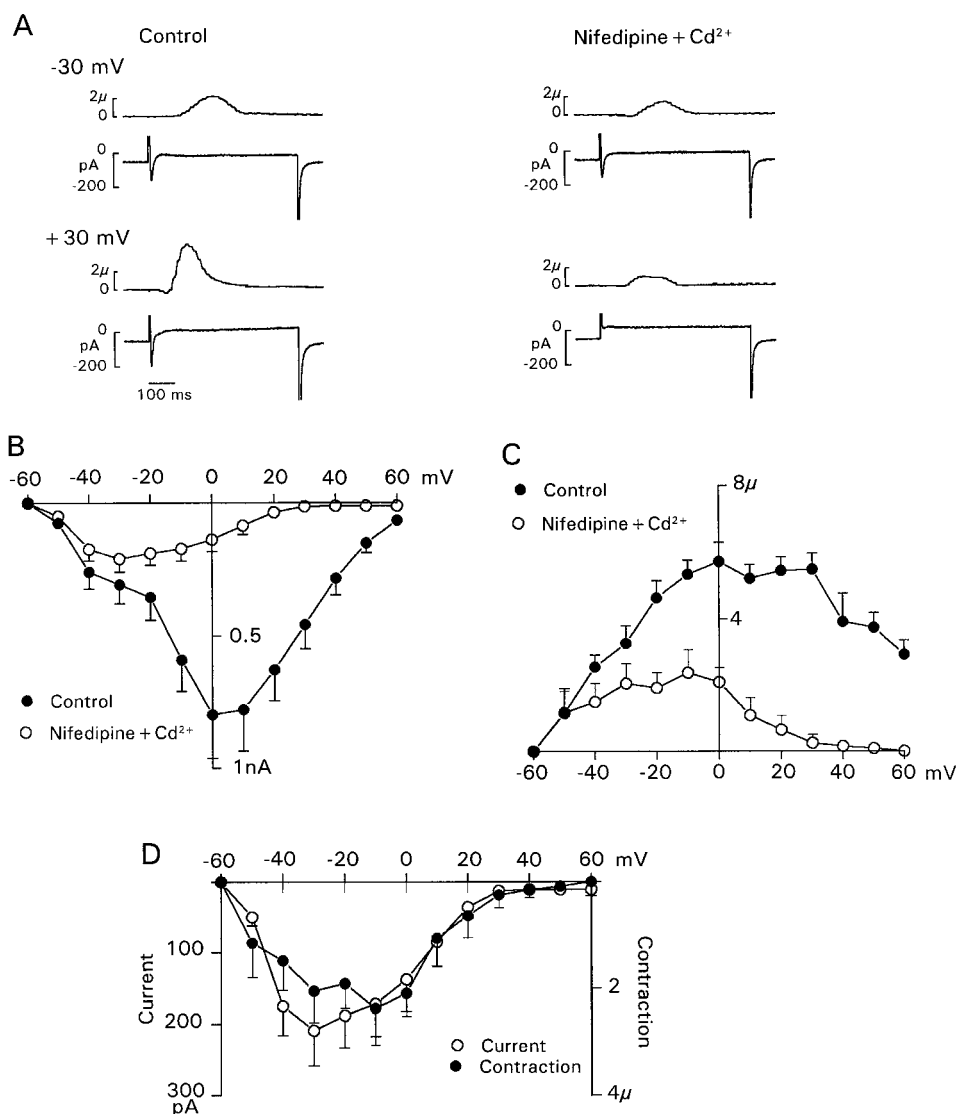


**FIGURE 4** Effect of nifedipine and low concentrations of  $\text{Cd}^{2+}$  on peak  $\text{Ca}^{2+}$  currents and cell shortening. (A) Original experimental records of  $\text{Ca}^{2+}$  current and cell shortening for voltage steps from  $-80$  to  $-30$  mV (to elicit T-type  $\text{Ca}^{2+}$  current) or  $+30$  mV (to elicit mostly L-type  $\text{Ca}^{2+}$  current). The addition of  $10 \mu\text{M}$  nifedipine plus  $10 \mu\text{M}$   $\text{Cd}^{2+}$  abolished L-type  $\text{Ca}^{2+}$  current with only a small reduction in T-type  $\text{Ca}^{2+}$  current amplitude. (B and C) Averaged data (mean  $\pm$  SEM) from four cells. (B) Peak  $I$ - $V$  plot for  $\text{Ca}^{2+}$  currents for control conditions and after the addition of nifedipine and  $\text{Cd}^{2+}$ . (C) Peak shortening-voltage relationships for the same conditions in the same cells. (D) The  $I$ - $V$  and peak shortening-voltage plots obtained in the presence of the nifedipine and  $\text{Cd}^{2+}$  drug combination are replotted and superimposed. The voltage dependence of the T-type  $\text{Ca}^{2+}$  current amplitude and peak shortening is similar. See text.

the addition of the combination of nifedipine and  $\text{Cd}^{2+}$  resulted from  $\text{Ca}^{2+}$  entry through T-type  $\text{Ca}^{2+}$  channels.

### Charge entry and cell shortening

We studied the amount of charge entering the cell as  $\text{Ca}^{2+}$  via T- or L-type channels and its ability to initiate cell contraction. Fig. 6 shows data from one cell. The cell was voltage clamped from the holding potential of  $-80$  mV to  $-30$  mV to elicit T-type  $\text{Ca}^{2+}$  current or to  $+40$  mV to elicit mostly L-type  $\text{Ca}^{2+}$  current, and the records were superimposed. Despite the smaller amplitude of the L-type  $\text{Ca}^{2+}$  current transient (compared with the T-type  $\text{Ca}^{2+}$  current transient), the cell contractions elicited by L-type  $\text{Ca}^{2+}$  current were of larger amplitude. In addition, the contraction was initiated after a shorter delay, had a more rapid rate of shortening and relaxation, and reached peak shortening earlier (see also Figs. 2 and 3). These findings suggest that, although  $\text{Ca}^{2+}$  entry by either T- or L-type channels is capable of initiating cell shortening,  $\text{Ca}^{2+}$  entry

through the L-type channel is a more effective trigger for cell shortening than is  $\text{Ca}^{2+}$  entry through the T-type channel.

We then calculated the amount of charge entering the cell during  $\text{Ca}^{2+}$  current transients for five cells having large-amplitude T-type  $\text{Ca}^{2+}$  currents. The voltage clamp protocol shown in Fig. 6 was used, and current traces for voltage steps from  $-80$  mV to  $-30$  mV (to elicit T-type  $\text{Ca}^{2+}$  current) or to  $+40$  mV (to elicit mostly L-type  $\text{Ca}^{2+}$  current) were analyzed. Charge was calculated by drawing a horizontal line through the current trace after decay of the inward  $\text{Ca}^{2+}$  current transient, and the area defined by that line and the  $\text{Ca}^{2+}$  current trace was integrated to provide an estimate of charge entry. Simultaneously recorded shortening records were analyzed for the delay to the onset of contraction, peak shortening, time to peak shortening, and maximal rate of shortening. These data are shown in Table 1. They indicate that, for voltage steps to  $-30$  mV or  $+40$  mV, the peak  $\text{Ca}^{2+}$  current amplitude and total charge were greater for the voltage step to  $-30$  mV, whereas peak shortening was greater and was reached earlier for the

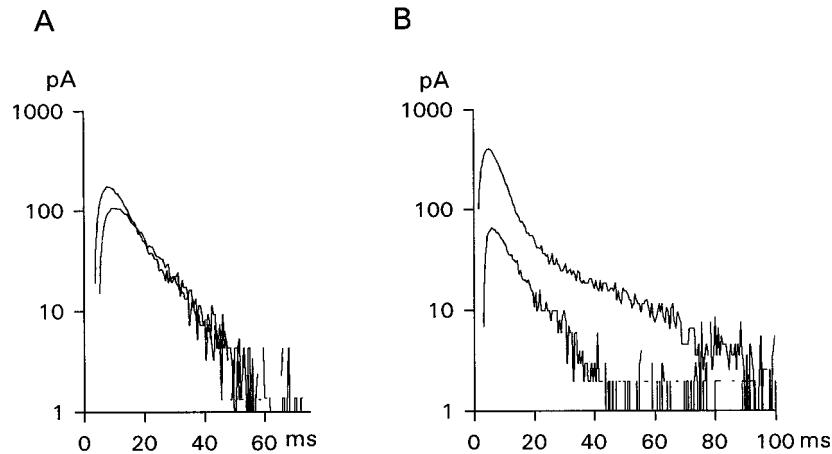


FIGURE 5 Effect of 10  $\mu\text{M}$  nifedipine plus 10  $\mu\text{M}$   $\text{Cd}^{2+}$  on the amplitude and decay characteristics of T- and L-type  $\text{Ca}^{2+}$  current. Each panel shows two current traces plotted as logarithmic transforms. (A) The depolarizing voltage steps were to  $-30$  mV to activate T-type  $\text{Ca}^{2+}$  current. (B) The depolarizing voltage steps were to 0 mV to activate both T-type and L-type  $\text{Ca}^{2+}$  current. In each panel, the larger amplitude current was recorded under control conditions and the smaller amplitude current was recorded after exposure to nifedipine and  $\text{Cd}^{2+}$ -containing bath solution. A shows that the current decays were linear and the drug combination had no effect on T-type  $\text{Ca}^{2+}$  current except to reduce slightly the amplitude. B shows that the addition of nifedipine and  $\text{Cd}^{2+}$  markedly reduced the current amplitude and converted the current decay to a single exponential process, consistent with block of L-type  $\text{Ca}^{2+}$  current leaving T-type  $\text{Ca}^{2+}$  channels unblocked.

voltage step to  $+40$  mV ( $p < 0.05$  for each comparison). The reduced time to peak shortening was the result of a decrease in the delay to the onset of contraction as well as an increased rate of shortening. These data provide quantitative support for the postulate that  $\text{Ca}^{2+}$  entry through the L-type channel, even when small, is more effective than

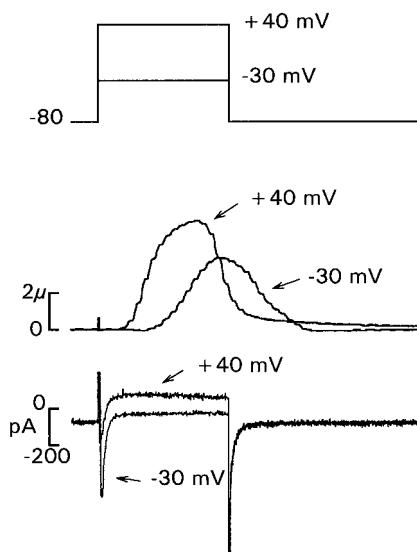


FIGURE 6 Charge entry and cell shortening. Voltage clamp steps were applied to  $-30$  mV to elicit T-type  $\text{Ca}^{2+}$  current or to  $+40$  mV to elicit mostly L-type  $\text{Ca}^{2+}$  current, and cell shortening was recorded simultaneously. Records are superimposed. Despite the larger T-type  $\text{Ca}^{2+}$  current amplitude and charge entry, cell contraction elicited by T-type  $\text{Ca}^{2+}$  current had a longer delay to onset, slower rate of shortening and relaxation, lower peak shortening, and longer time to peak shortening. The holding potential was  $-80$  mV.

$\text{Ca}^{2+}$  entry through the T-type channel in initiating a contraction.

### Source of activator $\text{Ca}^{2+}$

We studied the role of the SR  $\text{Ca}^{2+}$  release using ryanodine to deplete SR  $\text{Ca}^{2+}$  stores (see Bers, 1991). An example record of the effect of ryanodine is shown in Fig. 7. From a holding potential of  $-80$  mV, clamp steps were applied to  $-40$  or  $+10$  mV to elicit T- or mostly L-type  $\text{Ca}^{2+}$  current, respectively, and cell shortening. After the addition of ryanodine ( $5$   $\mu\text{M}$ ) to the bath, cell shortening was rapidly abolished, suggesting dependence on SR  $\text{Ca}^{2+}$  release. Ryanodine had no effect on the underlying T-type  $\text{Ca}^{2+}$  current whereas L-type  $\text{Ca}^{2+}$  current amplitude was slightly increased and the current decay was slowed (for discussion, see Balke and Weir, 1991). Similar results were observed in four cells exposed to  $1$ – $5$   $\mu\text{M}$  ryanodine. We also studied the effect of the membrane permeant  $\text{Ca}^{2+}$  chelator BAPTA-AM to buffer cell  $\text{Ca}^{2+}$  (Tsien, 1981). BAPTA-AM ( $100$   $\mu\text{M}$ ) exposure also resulted in the disappearance of cell shortening with little effect on the  $\text{Ca}^{2+}$  currents (data not shown). These findings support the conclusion that  $\text{Ca}^{2+}$  entry by T- or L-type  $\text{Ca}^{2+}$  channels leads to the initiation of contraction by the release of additional  $\text{Ca}^{2+}$  from the SR.

### DISCUSSION

In the mammalian heart, the initiation of each contraction is thought to result from  $\text{Ca}^{2+}$  influx through voltage-gated, sarcolemmal L-type  $\text{Ca}^{2+}$  channels, and possibly the Na-Ca exchange mechanism, to initiate the release of additional

**TABLE 1** Characteristics of T- and L-type  $\text{Ca}^{2+}$  currents and cell shortening

Voltage step amplitude	Peak $\text{Ca}^{2+}$ current (pA)	Total charge (fC)	Peak shortening ( $\mu\text{m}$ )	Time to peak shortening (ms)	Delay to onset of shortening (ms)
-30 mV	$568 \pm 70$	$6642 \pm 1120$	$3.7 \pm 0.4$	$355 \pm 50$	$116 \pm 13$
+40 mV	$300 \pm 56^*$	$4267 \pm 371^*$	$4.9 \pm 0.6^*$	$233 \pm 10^*$	$68 \pm 5^*$

Steps to -30 mV elicited T-type  $\text{Ca}^{2+}$  current. Steps to +40 mV elicited mostly L-type  $\text{Ca}^{2+}$  current. The onset of shortening was defined as the point of initiation of continuously increasing sampled digital values. Delay to onset of shortening and time to peak shortening were measured from the time of application of the voltage clamp step.

\* $P < 0.05$  when compared at the two voltages (Student's t-test). Data are presented as mean  $\pm$  SEM.

$\text{Ca}^{2+}$  from the SR. An important finding in the present work is that under our experimental conditions  $\text{Ca}^{2+}$  entry through T-type  $\text{Ca}^{2+}$  channels also can induce cell contraction, and these are the first experiments to show this directly.

Our findings show that  $\text{Ca}^{2+}$  entry via T-type  $\text{Ca}^{2+}$  channels, as with L-type  $\text{Ca}^{2+}$  channels, does not induce cell shortening by interacting directly with myofilaments. Rather, the initiation of contraction by T-type  $\text{Ca}^{2+}$  channels depends on  $\text{Ca}^{2+}$  release from the SR. This conclusion is supported most strongly by the experiments employing ryanodine to deplete SR  $\text{Ca}^{2+}$ . Despite the persistence of robust T-type  $\text{Ca}^{2+}$  currents under these conditions, cell shortening was abolished, and similar findings were obtained with BAPTA-AM. Comparable findings were obtained for L-type  $\text{Ca}^{2+}$  current with ryanodine and BAPTA-AM. We conclude that the mechanism of  $\text{Ca}^{2+}$ -induced  $\text{Ca}^{2+}$  release from the SR underlies the contraction induced by  $\text{Ca}^{2+}$  entry through both T- and L-type  $\text{Ca}^{2+}$  channels.

Although  $\text{Ca}^{2+}$  entry through T- and L-type  $\text{Ca}^{2+}$  channels can initiate contraction, the properties measured for the

contractions are different.  $\text{Ca}^{2+}$  entry via L-type  $\text{Ca}^{2+}$  channels consistently produced larger amplitude and faster contractions. In contrast,  $\text{Ca}^{2+}$  entry through T-type  $\text{Ca}^{2+}$  channels activated cell shortening after a longer delay, the rates of shortening and relaxation were reduced, peak shortening amplitude was less, and time to peak shortening amplitude was increased. Even when peak  $\text{Ca}^{2+}$  current amplitude and charge entry were greater through T-type  $\text{Ca}^{2+}$  channels, the cell shortening differences persisted. Taken together, these observations suggest that  $\text{Ca}^{2+}$  entry through the T-type  $\text{Ca}^{2+}$  channel is a less effective signal transduction mechanism for SR  $\text{Ca}^{2+}$  release and cell shortening than is  $\text{Ca}^{2+}$  entry through the L-type  $\text{Ca}^{2+}$  channel.

It is important to understand the distribution and physical properties of T- and L-type  $\text{Ca}^{2+}$  channels, and their relationships to SR  $\text{Ca}^{2+}$  release channels, in considering models of E-C coupling that may explain our results. In ventricular muscle, where most E-C coupling experimental work has been performed, contraction results from the opening of sarcolemmal (mostly in t-tubules) L-type  $\text{Ca}^{2+}$  channels, which causes localized  $\text{Ca}^{2+}$  accumulation and activation of associated SR  $\text{Ca}^{2+}$  release channel(s). This local control of intracellular  $\text{Ca}^{2+}$  and SR  $\text{Ca}^{2+}$  release is facilitated by the close physical proximity of L-type  $\text{Ca}^{2+}$  channels and SR  $\text{Ca}^{2+}$  release channels in dyads, and  $\text{Ca}^{2+}$  release is then controlled by the L-type  $\text{Ca}^{2+}$  channel unitary current (for discussion, see Wibo et al., 1990; Cleemann and Morad, 1991; Stern, 1992; Weir et al., 1994; Carl et al., 1995; Sham et al., 1995; G6mes et al., 1997). Extending these observations to cardiac Purkinje cells must be done with care. In Purkinje cells, where only a rudimentary t-tubule network exists,  $\text{Ca}^{2+}$  channels are located on the cell surface. Single-channel studies of T- and L-type  $\text{Ca}^{2+}$  channels in Purkinje cells have shown that many patches contain both channel types; hence marked spatial segregation seems not to occur (Shorofsky and January, 1992). The unitary conductances for  $\text{Ca}^{2+}$  of these T- and L-type  $\text{Ca}^{2+}$  channels is similar, although differences existed in channel gating properties. If  $\text{Ca}^{2+}$  entering by T- and L-type  $\text{Ca}^{2+}$  channels had equal access to the SR  $\text{Ca}^{2+}$  release channel, then  $\text{Ca}^{2+}$  entering the cell by the T-type  $\text{Ca}^{2+}$  channel might be expected to be equally effective in initiating cell contraction. Our experimental results do not show this. Rather, our findings show that it is  $\text{Ca}^{2+}$  entry through L-type  $\text{Ca}^{2+}$  channels that is more effective at initiating cell contraction. One explanation for our data is that  $\text{Ca}^{2+}$  entry

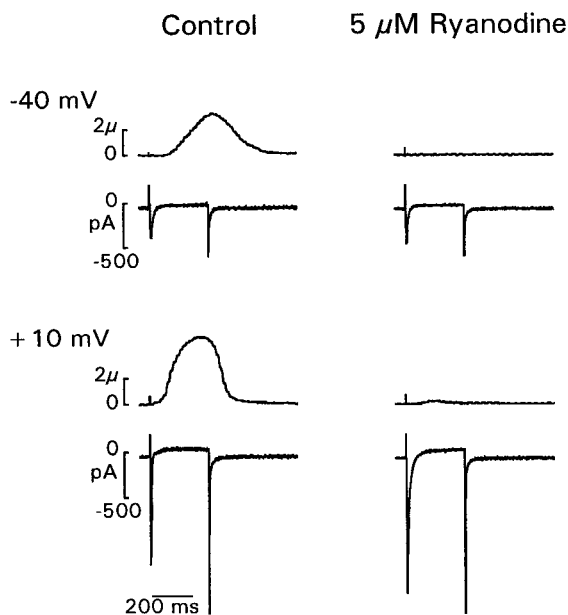


**FIGURE 7** Effect of ryanodine. T- and L-type  $\text{Ca}^{2+}$  currents and cell shortening were elicited by clamp steps to -40 or +10 mV, respectively. Ryanodine (5  $\mu\text{M}$ , 11 min of exposure) abolished cell contractions, suggesting dependence on SR  $\text{Ca}^{2+}$  release. The holding potential was -80 mV.



through the L-type  $\text{Ca}^{2+}$  channel in cardiac Purkinje cells, compared with the T-type  $\text{Ca}^{2+}$  channel, has preferential access to the SR  $\text{Ca}^{2+}$  release mechanism. One possibility is that L-type  $\text{Ca}^{2+}$  channels are in close proximity to SR  $\text{Ca}^{2+}$  release channels, whereas T-type  $\text{Ca}^{2+}$  channels are located at a greater or more variable distance from SR  $\text{Ca}^{2+}$  release channels, and the decreased effectiveness arises from longer and more variable  $\text{Ca}^{2+}$  diffusion distances as well as increased intracellular  $\text{Ca}^{2+}$  buffering. Our experiments, however, do not address the molecular mechanism linking L-type  $\text{Ca}^{2+}$  channels to the SR  $\text{Ca}^{2+}$  release process in Purkinje cells, and whether this is similar to the local control mechanism postulated for ventricular muscle.

Several limitations exist with our experiments. 1) Our results were obtained in cardiac Purkinje cells. These cells differ structurally and functionally from ventricular cells, which are the most commonly studied cell model for cardiac E-C coupling; thus, extrapolation of our findings to ventricular cells must be performed cautiously. 2) These experiments were performed under  $\text{Na}^+$ -free conditions (with tetrodotoxin present), which is essential for studying T-type  $\text{Ca}^{2+}$  current. Although efforts were made to minimize the potential of cell  $\text{Ca}^{2+}$  loading, we cannot exclude an effect from this. 3) A role has been suggested in cardiac cell E-C coupling for the reverse mode of the electrogenic Na-Ca exchange mechanism, responding to membrane depolarization and local changes in the  $\text{Na}^+$  gradient near the  $\text{Na}^+$  channel, in mediating  $\text{Ca}^{2+}$  entry into cells to initiate contraction (Bers et al., 1988; Leblanc and Hume, 1990; Nuss and Houser, 1992; Lipp and Niggli, 1994; Kohomoto et al., 1994; Wasserstrom and Vites, 1996; but see Sham et al., 1992; Bouchard et al., 1993). In our experiments,  $\text{Na}^+$  was absent from the internal pipette and bath solutions during experiments. Previous studies performed under similar experimental conditions have shown that  $\text{Ca}^{2+}$  entry by the Na-Ca exchange mechanism is inhibited, presumably because the intracellular  $\text{Na}^+$  concentration becomes very low (Cannell et al., 1986; Bers et al., 1990; Weir et al., 1994). This suggests that  $\text{Ca}^{2+}$  entry through the Na-Ca exchange mechanism is unlikely in our experiments, although we cannot exclude completely a role for this, particularly at more positive voltages. 4) The potential for cooperative effects between T- and L-type  $\text{Ca}^{2+}$  channel types exists, a point not addressed by our experiments. 5) We did not measure directly intracellular free  $\text{Ca}^{2+}$ . However, in a recent brief report, Sipido and Carmeliet (1996) showed that T-type  $\text{Ca}^{2+}$  channel activation in guinea pig ventricular cells could lead to  $\text{Ca}^{2+}$  release from the SR. Interestingly, they reported that  $\text{Ca}^{2+}$  entry via the T-type  $\text{Ca}^{2+}$  channel was a less efficient mechanism than the L-type  $\text{Ca}^{2+}$  channel for triggering  $\text{Ca}^{2+}$  release from the SR.

In summary, these experiments were intended to investigate whether T-type  $\text{Ca}^{2+}$  channels could contribute to cardiac cell contraction. Our results provide strong evidence that  $\text{Ca}^{2+}$  entry by T-type  $\text{Ca}^{2+}$  channels can initiate cell contraction in cardiac Purkinje cells and that the contractions depend on  $\text{Ca}^{2+}$ -induced  $\text{Ca}^{2+}$  release from the SR.

$\text{Ca}^{2+}$  entry as L-type  $\text{Ca}^{2+}$  current, however, initiated larger amplitude and more rapid contractions than  $\text{Ca}^{2+}$  entry as T-type  $\text{Ca}^{2+}$  current. Hence, we conclude that the L-type  $\text{Ca}^{2+}$  channel is a more effective signal transduction mechanism to the SR  $\text{Ca}^{2+}$  release channel in our experiments. What is the role of T-type  $\text{Ca}^{2+}$  channels in E-C coupling in other heart cell types? In a normal ventricular cell, under physiological conditions, where T-type  $\text{Ca}^{2+}$  current amplitude is small, our results suggest that  $\text{Ca}^{2+}$  entry through T-type  $\text{Ca}^{2+}$  channels is likely to play little direct role in E-C coupling. Our findings may have greater significance, however, for the regulation of contraction in cardiac cell types with larger T-type  $\text{Ca}^{2+}$  channel densities such as atrial cells, and potentially in postnatal or pathological settings where T-type  $\text{Ca}^{2+}$  current expression is enhanced, or in heart diseases where the L-type  $\text{Ca}^{2+}$  channel local control mechanism becomes impaired (Gómes et al., 1997).

We thank Drs. Timothy Kamp and Hector Valdivia for careful review of the manuscript. We also thank Dr. Harry Fozzard for his enthusiastic support of this work.

This study was supported in part by National Heart, Lung, and Blood Institute grant HL 38927 and by the Oscar Rennebohm Foundation at the University of Wisconsin. Dr. Zhou received partial support by a Fellowship Award from the Metropolitan Chicago American Heart Association.

## REFERENCES

- Balke, C. W., and W. G. Weir. 1991. Ryanodine does not affect calcium current in guinea pig ventricular myocytes in which  $\text{Ca}^{2+}$  is buffered. *Circ. Res.* 68:897-902.
- Barry, P. H., and J. P. Calc. 1994. A software package for calculating liquid junction potential corrections in patch-clamp, intracellular, epithelial and bilayer measurements and for correcting junction potential measurements. *J. Neurosci. Methods.* 51:107-116.
- Bean, B. P. 1984. Nitrendipine block of cardiac calcium channels: high affinity binding to the inactivated state. *Proc. Natl. Acad. Sci. U.S.A.* 81:6388-6392.
- Bean, B. P. 1985. Two kinds of calcium channels in canine atrial cells: differences in kinetics, selectivity, and pharmacology. *J. Gen. Physiol.* 86:1-30.
- Bers, D. M. 1991. Excitation-Contraction Coupling and Cardiac Contractile Force. Kluwer Academic Publishers, Dordrecht, The Netherlands.
- Bers, D. M., D. M. Christensen, and T. X. Nguyen. 1988. Can Ca entry via Na-Ca exchange directly activate cardiac muscle contraction. *J. Mol. Cell. Cardiol.* 20:405-414.
- Bers, D. M., W. J. Lederer, and J. R. Berlin. 1990. Intracellular Ca transients in rat cardiac myocytes: role of Na-Ca exchange, the calcium current, and the sarcoplasmic reticulum. *Am. J. Physiol.* 258: C944-C954.
- Bouchard, R. A., R. B. Clark, and W. R. Giles. 1993. Role of sodium-calcium exchange in activation of contraction in rat ventricle. *J. Physiol.* 472:391-413.
- Callewaert, G. 1992. Excitation-contraction coupling in mammalian cardiac cells. *Cardiovasc. Res.* 26:923-932.
- Cannell, M. B., D. A. Eisner, W. J. Lederer, and M. Valdeolmillos. 1986. Effect of membrane potential on intracellular calcium concentration in sheep Purkinje fibers in sodium-free solutions. *J. Physiol.* 381:193-203.
- Carl, S. L., K. Felix, A. H. Caswell, N. R. Brandt, W. J. Ball, P. L. Vaghy, G. Meissner, and D. G. Ferguson. 1995. Immunolocalization of sarcolemmal dihydropyridine receptor and sarcoplasmic reticular triadin and ryanodine receptor in rabbit ventricle and atrium. *J. Cell Biol.* 129:672-682.

- Cleemann, L., and M. Morad. 1991. Role of  $\text{Ca}^{2+}$  channel in cardiac excitation-contraction coupling in the rat: evidence from  $\text{Ca}^{2+}$  transients and contraction. *J. Physiol.* 432:283–312.
- Fares, N., J. P. Gomez, and D. Potreau. 1996. T-type calcium current is expressed in dedifferentiated adult rat ventricular cells in primary culture. *Comptes Rendus Acad. Sci. Ser. III Sci. Vie Life Sci.* 319:569–576.
- Gómes, A. M., H. H. Valdivia, H. Cheng, M. R. Lederer, L. F. Santana, M. B. Cannell, S. A. McCune, R. A. Altschuld, and W. J. Lederer. 1997. Defective excitation-contraction coupling in experimental cardiac hypertrophy and heart failure. *Science.* 276:800–806.
- Hagiwara, N., H. Irisawa, and M. Kameyama. 1988. Contribution of two types of calcium currents to the pacemaker potentials of rabbit sino-atrial node cells. *J. Physiol.* 395:233–253.
- Hirano, Y., H. A. Fozzard, and C. T. January. 1989a. Characteristics of L- and T-type  $\text{Ca}^{2+}$  currents in canine cardiac Purkinje cells. *Am. J. Physiol.* 256:H1478–H1492.
- Hirano, Y., H. A. Fozzard, and C. T. January. 1989b. Inactivation properties of T-type calcium current in canine cardiac Purkinje cells. *Biophys. J.* 56:1007–1016.
- Hirano, Y., A. Moscucci, and C. T. January. 1992. Direct measurement of L-type  $\text{Ca}^{2+}$  window current in heart cells: separation from slowly inactivating current. *Circ. Res.* 70:445–455.
- Horn, R., and A. Marty. 1988. Muscarinic activation of ionic currents measured by a new whole-cell recording method. *J. Gen. Physiol.* 92:145–159.
- January, C. T., and H. A. Fozzard. 1990. Role for sodium channels and intracellular sodium in the regulation of the cardiac force-frequency relation and contractility. In *Subcellular Basis of Contractile Failure*. B. Korecky and N. S. Dhalla, editors. Kluwer Academic Publishers, Dordrecht, The Netherlands. 3–17.
- Kamp, T. J., Z. Zhou, J. C. Makielski, and C. T. January. 1998. The pharmacology of T- and L-type calcium channels in the heart. In *Cardiac Electrophysiology: From Cell to Bedside*. 3rd ed. J. Jalife and D. Zipes, editors. W.B. Saunders. In press.
- Kohmoto, O., A. J. Levi, and J. H. B. Bridge. 1994. Relation between reverse sodium-calcium exchange and sarcoplasmic reticulum calcium release in guinea pig ventricular cells. *Circ. Res.* 73:550–554.
- Le Grand, B., E. Deroubaix, A. Coulombe, and E. Coraboeuf. 1990. Stimulatory effect of ouabain on T- and L-type calcium currents in guinea pig cardiac myocytes. *Am. J. Physiol.* 258:H1620–H1623.
- Leblanc, N., and J. R. Hume. 1990. Sodium current-induced release of calcium from cardiac sarcoplasmic reticulum. *Science.* 248:372–376.
- Lipp, P., and E. Niggli. 1994. Sodium current-induced calcium signals in isolated guinea-pig ventricular myocytes. *J. Physiol.* 474:439–446.
- McDonald, T. F., D. Pelzer, and W. Trautwein. 1984. Cat ventricular muscle treated with D600: characteristics of calcium channel block and unblock. *J. Physiol.* 352:217–241.
- McDonald, T. F., S. Pelzer, W. Trautwein, and D. J. Pelzer. 1994. Regulation and modulation of calcium channels in cardiac, skeletal, and smooth muscle cells. *Physiol. Rev.* 74:365–507.
- Mitra, R., and M. Morad. 1986. Two types of calcium channels in guinea pig ventricular myocytes. *Proc. Natl. Acad. Sci. U.S.A.* 83:5340–5344.
- Nilius, B., P. Hess, J. B. Lansman, and R. W. Tsien. 1985. A novel type of cardiac calcium channel in ventricular cells. *Nature.* 316:443–446.
- Nuss, H. B., and S. R. Houser. 1992. Sodium-current exchange-mediated contractions in feline ventricular myocytes. *Am. J. Physiol.* 263: H1161–H1169.
- Nuss, H. B., and S. R. Houser. 1993. T-type  $\text{Ca}^{2+}$  current is expressed in hypertrophied adult feline left ventricular myocytes. *Circ. Res.* 73: 777–782.
- Rae, J., K. Cooper, G. Gates, and M. Watsky. 1990. Low access resistance perforated patch recordings using amphotericin B. *J. Neurosci. Methods.* 37:15–26.
- Sanguinetti, M. C., and R. S. Kass. 1984. Voltage-dependent block of calcium channel current in calf cardiac Purkinje fibers by dihydropyridine calcium channel antagonists. *Circ. Res.* 55:336–348.
- Sen, L., and T. W. Smith. 1994. T-type  $\text{Ca}^{2+}$  channels are abnormal in genetically determined cardiomyopathic hamster hearts. *Circ. Res.* 75: 149–155.
- Sham, J. S. K., L. Cleemann, and M. Morad. 1992. Gating of the cardiac  $\text{Ca}^{2+}$  release channel: the role of  $\text{Na}^{+}$  current and  $\text{Na}^{+}$ - $\text{Ca}^{2+}$  exchange. *Science.* 255:850–853.
- Sham, J. S., L. Cleemann, and M. Morad. 1995. Functional coupling of  $\text{Ca}^{2+}$  channels and ryanodine receptors in cardiac myocytes. *Proc. Natl. Acad. Sci. U.S.A.* 92:121–125.
- Sheets, M. F., C. T. January, and H. A. Fozzard. 1983. Isolation and characterization of single canine cardiac Purkinje cells. *Circ. Res.* 53: 544–548.
- Shorofsky, S. R., and C. T. January. 1992. L- and T-type  $\text{Ca}^{2+}$  channels in canine cardiac Purkinje cells: single-channel demonstration of L-type  $\text{Ca}^{2+}$  window current. *Circ. Res.* 70:456–464.
- Sipido, K. R., and E. Carmeliet. 1996. Can  $\text{Ca}^{2+}$  entry through T-type  $\text{Ca}^{2+}$  channels trigger  $\text{Ca}^{2+}$  release from the sarcoplasmic reticulum in guinea-pig ventricular myocytes? *Biophys. J.* 70:A245.
- Spurgeon, H. A., M. D. Stern, G. Baartz, S. Raffaelli, R. G. Hansford, A. Talo, E. G. Lakatta, and M. C. Capogrossi. 1990. Simultaneous measurement of  $\text{Ca}^{2+}$ , contraction, and potential in cardiac myocytes. *Am. J. Physiol.* 258:H574–H586.
- Steadman, B. W., K. B. Moore, K. W. Spitzer, and J. H. B. Bridge. 1988. A video system for measuring motion in contraction heart cells. *IEEE Trans. Biomed. Eng.* 35:264–272.
- Stern, M. D. 1992. Theory of excitation-contraction coupling in cardiac muscle. *Biophys. J.* 63:497–517.
- Tseng, G., and A. Boyden. 1989. Multiple types of  $\text{Ca}^{2+}$  currents in single canine Purkinje cells. *Circ. Res.* 65:1735–1750.
- Tsien, R. Y. 1981. A non-disruptive technique for loading calcium buffers and indicators into cells. *Nature.* 290:527–528.
- Vorperian, V. R., Z. Zhou, S. Mohammad, T. J. Hoon, C. Studenik, and C. T. January. 1996. Torsades de pointes with an antihistamine metabolite: potassium channel block with desmethylastemizole. *J. Am. Coll. Cardiol.* 28:1556–1561.
- Wasserstrom, J. A., and A. M. Vites. 1996. The role of  $\text{Na}^{+}$ - $\text{Ca}^{2+}$  exchange in activation of excitation-contraction coupling in rat ventricular myocytes. *J. Physiol.* 493:529–542.
- Wibo, M., G. Bravo, and T. Godfraind. 1990. Postnatal maturation of excitation-contraction coupling in rat ventricle in relation to the subcellular localization and surface density of 1,4-dihydropyridine and ryanodine receptors. *Circ. Res.* 68:662–673.
- Weir, W. G., T. M. Egan, J. R. Lopez-Lopez, and C. W. Balke. 1994. Local control of excitation-contraction coupling in rat heart cells. *J. Physiol.* 474:463–471.
- Xu, X., and P. M. Best. 1992. Postnatal changes in T-type calcium current density in rat atrial myocytes. *J. Physiol.* 454:657–672.
- Zhou, Z., and S. L. Lipsius. 1994. T-type calcium current in latent pacemaker cells isolated from cat right atrium. *J. Mol. Cell. Cardiol.* 26: 1211–1219.
- Zhou, Z., C. Studenik, and C. T. January. 1995. Properties of E-4031-induced early afterdepolarizations in rabbit ventricular myocytes: studies using a perforated patch method. In *Potassium Channels in Normal and Pathological Conditions*. J. Vereecke, P. P. van Bogaert, and F. Verdonck, editors. Leuven University Press, Leuven, The Netherlands. 375–379.